

CORRELATION BETWEEN STRUCTURE AND THE MAGNETIC PROPERTIES OF AMORPHOUS AND NANOCRYSTALLINE $\text{Fe}_{74}\text{Cu}_{0.5}\text{Nb}_3\text{Si}_{13.5}\text{B}_9$ ALLOYS

SIBA P. MONDAL¹, KAZI HANIUM MARIA^{*2}, S.S. SIKDER¹, SHIREEN AKHTER³, M.A. HAKIM³ AND SHAMIMA CHOUDHURY²

Department of Physics, Khulna University of Engineering & Technology, Khulna-9203, Bangladesh

ABSTRACT

Structural and magnetic measurements have been performed on the FINEMET type of ribbons with nominal composition of $\text{Fe}_{74}\text{Cu}_{0.5}\text{Nb}_3\text{Si}_{13.5}\text{B}_9$ synthesized by rapid solidification technique. The crystallization behavior and the nanocrystal formation have been studied by differential thermal analysis (DTA) and X-ray diffraction (XRD). The crystallization onset temperatures determined by XRD are in good agreement with DTA results. Magnetic permeability and magnetization measurements have been carried out using inductance analyzer and vibrating sample magnetometer (VSM). Magnetic permeability sensitively depends on the annealing temperature which increases sharply with the increase of annealing temperature. Maximum permeability corresponding to optimum annealing temperature (T_a) was observed at $T_a = 575^\circ\text{C}$. Saturation magnetization, M_s , increases with T_a for the sample and finally decreases for annealing at a temperature much higher than peak crystallization temperature. The results show that the amounts of Cu and Nb are very important for the soft magnetic properties of FINEMET alloys.

Key words: FINEMET, XRD, Grain size, Permeability, Saturation, Magnetization

INTRODUCTION

Over the past several decades, amorphous and more recently nanocrystalline materials have been investigated for applications in magnetic devices requiring magnetically soft materials such as transformers, inductive devices, etc. Most recently, research interest in nanocrystalline soft magnetic alloys has dramatically increased. The benefits found in the nanocrystalline alloys stem from their chemical and structural variations on a nanoscale which are important for developing optimal magnetic properties. Amorphous soft magnetic alloys are now well accepted as mature materials. The term “Nanocrystalline alloy” will be used for those alloys that have a majority of grain diameters in the typical range from $\approx 1 - 50$ nm. This term will include alloys made by rapid solidification, deposition techniques and solid state reactions, where the initial material may be in the amorphous state and subsequently crystallized. Nanocrystalline

^{*}Corresponding author :<kazimaria@univdhaka.edu>.

²Department of Physics, University of Dhaka, Dhaka -1000, Bangladesh

³Materials Science Division, Atomic Energy Centre, Dhaka – 1000, Bangladesh

soft magnetic materials were first reported in 1988 by Yoshizawa *et al.* (1988), Yoshizawa and Yamachi (1990), Noh *et al.* (1990) through controlled crystallization of Fe-Si-B amorphous alloys with the addition of copper (Cu) and niobium (Nb) which are known as FINEMET. The magnetic softness of FINEMET alloy mainly arises from the depression of ultrafine grains in an amorphous matrix which reduces the effective magnetic anisotropy and magnetostriction. This indicates that the exchange interaction between nanocrystalline and amorphous phases plays an important role in achieving good soft magnetic properties (Bigot *et al.* 1994, Manjura Hoque and Hakim 2007). The formation of these nanocrystalline structures is ascribed to the combined addition of Cu and Nb, which are not soluble in α -Fe. Hereby Cu is thought to increase the nucleation of α -Fe grains, whereas Nb hinders its growth rate (Yoshizawa and Yamachi 1991).

The aim of the present study was to observe structure and measure magnetic properties of $\text{Fe}_{74}\text{Cu}_{0.5}\text{Nb}_3\text{Si}_{13.5}\text{B}_9$ and find the correlation between them. Frequency dependence of permeability has been measured in the amorphous and nanocrystalline state with different volume fraction of amorphous and nanocrystalline phase.

MATERIALS AND METHODS

Amorphous ribbons with the nominal composition $\text{Fe}_{74}\text{Cu}_{0.5}\text{Nb}_3\text{Si}_{13.5}\text{B}_9$ were prepared in an arc furnace on a water-cooled copper hearth under an atmosphere of pure Ar. The purity of the constituent elements were, Fe (99.9%), Nb (99.9%), Si (99.9%), Cu (99.9%) and B (99.9%) and were obtained from Johnson Matthey (Alfa Aesar Inc.). Amorphousness of the ribbon and nanocrystalline structure have been observed by X-ray diffraction (Philips (PW 3040) X 'Pert PRO XRD) with Cu- K_{α} radiation. Crystallization behavior has been performed using Differential Scanning Calorimetry (2960 SDT, USA). Measurement of frequency dependence of initial permeability has been carried out by laboratory built furnace and Wayne Kerr 3255 B Impedance Analyzer. Temperature dependence of magnetization has been performed using 880 DMS Vibrating Sample Magnetometer, USA.

RESULTS AND DISCUSSION

Fig. 1 shows DTA profile of as-cast amorphous ribbons with a heating rate of $20^{\circ}\text{C}/\text{min}$ in a nitrogen atmosphere. Two exothermic peaks are distinctly observed which correspond to two different crystallization events at temperatures T_{x_1} and T_{x_2} , respectively. The soft magnetic properties correspond to the primary crystallization (T_{x_1}) of α -Fe (Si) phase. Secondary crystallization (T_{x_2}) corresponds to Fe-B phase which causes magnetic hardening of the nanocrystalline alloy. The crystallization onset temperatures (T_{x_1} and T_{x_2}) and peak temperatures (T_{p_1} and T_{p_2}) display exothermic peak, i.e. release of heat during the crystallization of Fe(Si) and Fe-B phases.

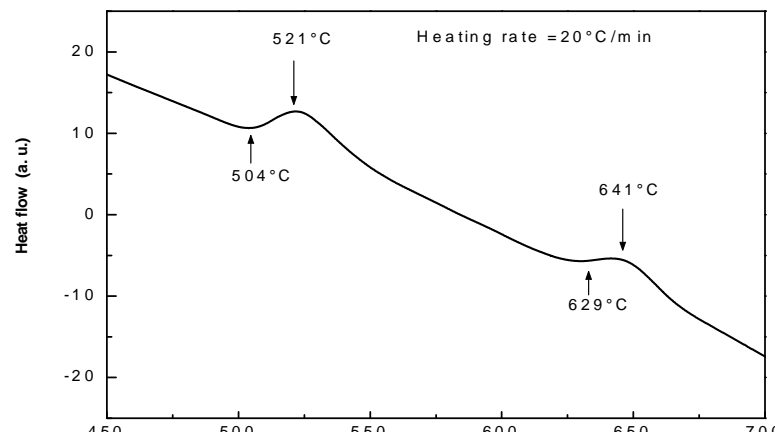


Fig. 1. DTA trace of the as-cast amorphous ribbon with composition $\text{Fe}_{74}\text{Cu}_{0.5}\text{Nb}_3\text{Si}_{13.5}\text{B}_9$ alloy with continuous heating.

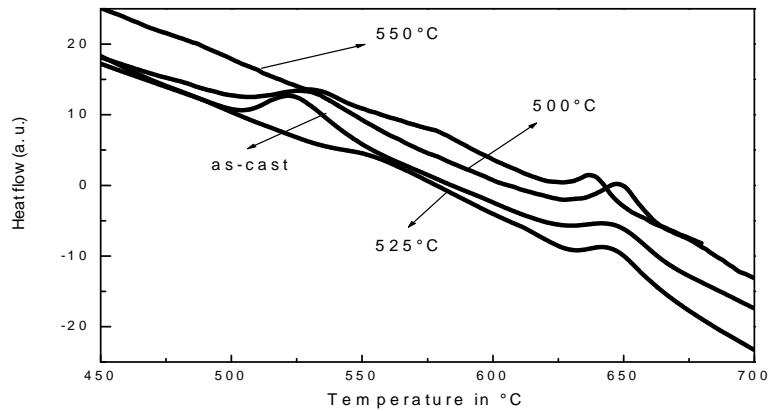


Fig. 2. Effects on DTA traces of as-cast and different annealing temperature on the nanocrystalline amorphous ribbon with composition $\text{Fe}_{74}\text{Cu}_{0.5}\text{Nb}_3\text{Si}_{13.5}\text{B}_9$.

The area under the first peak of DTA curve corresponds to the crystallization enthalpy, ΔH of Fe(Si) from which the volume fraction of crystallization (X_f) can be estimated according to the formula,

$$X_f = \frac{\Delta H_a - \Delta H_t}{\Delta H_a}, \quad (1)$$

where ΔH_a and ΔH_t are the crystallization enthalpy of the as-cast alloy and that of the alloy annealed for a time t , respectively. Fig. 2 shows DTA profiles of $\text{Fe}_{74}\text{Cu}_{0.5}\text{Nb}_3\text{Si}_{13.5}\text{B}_9$ alloy in the as cast state and annealed at different temperatures for 30 min. From the DTA scan, it is observed that the as-cast and annealed samples at $T_a = 500^\circ\text{C}$ do not show any significant change of area under the 1st peak corresponding to the crystallization enthalpy, ΔH of Fe(Si). This means that at $T_a = 500^\circ\text{C}$, no crystallization

occurred which is quite obvious since $T_{x_1} = 504^\circ\text{C}$ for this sample. This demonstrates that even annealing at $T_a = 500^\circ\text{C}$, the material still remained amorphous. Therefore crystallization enthalpy ΔH (area under the peak) is almost equal to that of its amorphous state. But when annealed at $T_a = 525^\circ\text{C}$, there is a broad diffused 1st peak meaning that substantial amount of primary crystallization, Fe(Si) has already been completed for 30 minutes at $T_a = 525^\circ\text{C}$. For $T_a = 550^\circ\text{C}$, 1st DTA peak is almost not visible, i.e. crystallization of Fe(Si) phase has almost completed. A critical scrutiny of 2nd peak does not show any significant change. This shows that with increasing annealing temperature X_f is expected to increase. The effect of annealing temperature T_a on the secondary crystallization is insignificant since the T_a is very low compared to T_{x_2} (Herzer 1989).

Table 1. Annealing effects on 1st and 2nd crystallization states of the nanocrystalline amorphous ribbon with composition $\text{Fe}_{74}\text{Cu}_{0.5}\text{Nb}_3\text{Si}_{13.5}\text{B}_9$ at constant heating rate $20^\circ\text{C}/\text{min}$.

Annealing temperature	Onset temp. of primary crystallization T_{x_1} °C	Primary crys. peak temperature T_{p_1} °C	Onset temp. of secondary crystallization T_{x_2} °C	Secondary crys. peak temperature T_{p_2} °C	(ΔT) $T_{p_2} - T_{x_1}$ in °C
As-cast	504	521	629	641	120
500°C	507	529	629	648	119
525°C	–	–	630	644	–
550°C	–	–	625	638	–

The results of DTA scan on annealing of sample together with as-cast sample with the parameter such as T_{x_1} , T_{x_2} , T_{p_1} , T_{p_2} and ΔT are depicted in Table 1. It is observed from the tables that the T_{x_1} , T_{x_2} , T_{p_1} , T_{p_2} as well as the difference between the two crystallization events are almost not affected by annealing, just below the crystallization temperatures. When the samples are annealed above the T_{p_1} , the primary crystallization as evidenced from their DTA curves are so diffused and smeared that they give signals of nearly completion of the primary crystallization of Fe(Si) crystallites.

XRD spectra of as-cast and annealed at 475 to 700°C for 30 minutes have been presented in Fig. 3. It is noticed that initiation of crystallization only takes place at $T_a = 525^\circ\text{C}$. Below this annealing temperature there is no sharp peak to indicate crystallization. The broad diffused peak around (110) plane necessarily signifies the amorphous state of the samples annealed at $T_a = 500^\circ\text{C}$ and below. XRD pattern clearly indicates the formation of bcc Fe(Si) phase above $T_a = 525^\circ\text{C}$ with the appearance of (110), (200) and (211) fundamental diffraction peaks. With the increasing of T_a , (110) diffraction peak becomes sharper which means that grains are growing bigger with the increase of annealing temperature. From Fig. 3 it is also observed that just below (110) peak, another diffraction line with small peak at $2\theta \approx 44^\circ$ appeared for the samples

annealed at $T_a = 650$ and 700°C . This diffraction line has been matched with Fe_{23}B_6 phase. Therefore the boride phase for this sample has appeared along with bcc Fe(Si).

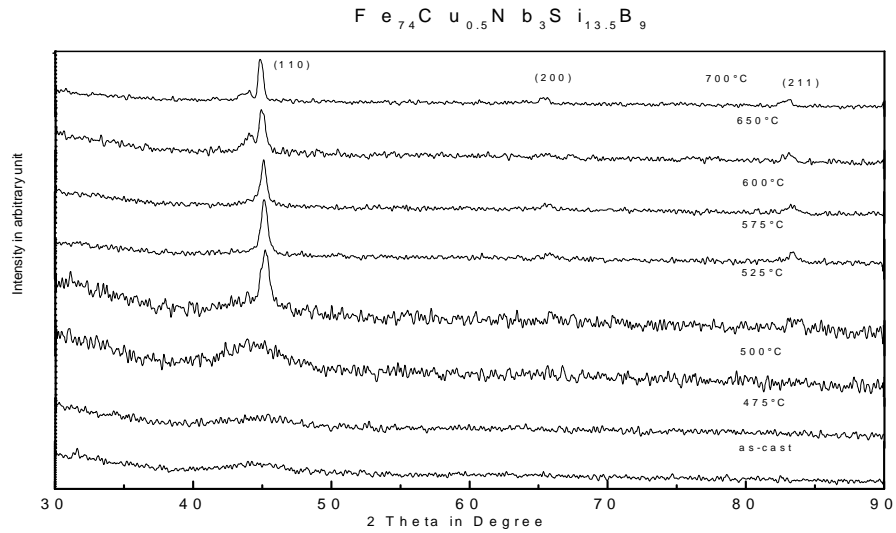


Fig. 3. XRD patterns of $\text{Fe}_{74}\text{Cu}_{0.5}\text{Nb}_3\text{Si}_{13.5}\text{B}_9$ alloys for as-cast and heat-treated at 475 to 700°C for 30 minutes.

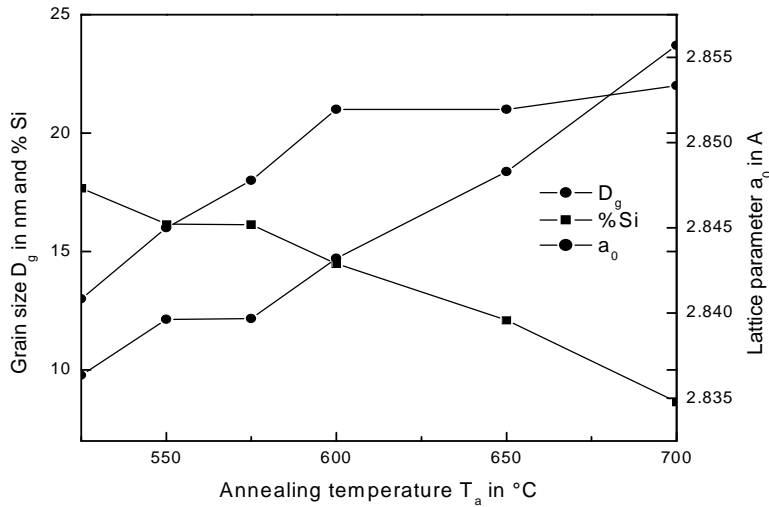


Fig. 4. Variation of D_g , a_0 and Si-content with T_a for the nanocrystalline amorphous ribbon with composition $\text{Fe}_{74}\text{Cu}_{0.5}\text{Nb}_3\text{Si}_{13.5}\text{B}_9$.

Fig. 4 shows the variation of lattice parameter of Fe(Si) phase, Si-content and grain size of α -Fe(Si) phase with respect to the annealing temperature of the samples. With the increase of annealing temperature, lattice parameter and grain size increases gradually

while Si content of Fe(Si) phase decreases with T_a . This is contradictory to original Finemet alloy. Such a situation may only be explained by assuming that at high temperature ($T > 500^\circ\text{C}$) recrystallization of Fe(Si) grains takes place. Lower Nb content may also be the reason this deviation. The real cause is not clear and remains still an open question. Enhancement of grain size with annealing temperature corresponds well with the reported results (Rubinstein *et al.* 2001). The formation of this particular nanostructure is ascribed to the combined effects of Cu and Nb and their low solubility in iron. All the results of θ , d-values, FWHM, a_0 , D_g and Si-content from XRD analysis are listed in Table 2.

Table 2. Experimental XRD data of nanocrystalline $\text{Fe}_{74}\text{Cu}_{0.5}\text{Nb}_3\text{Si}_{13.5}\text{B}_9$ amorphous ribbon at different annealing temperatures.

Temperature ($^\circ\text{C}$)	θ ($^\circ$)	d (\AA)	FWHM ($^\circ$)	a_0 (\AA)	D_g (nm)	Si (%)
525	22.604	2.005	0.70	2.8363	13	17.68
550	22.577	2.007	0.59	2.8396	16	16.15
575	22.576	2.007	0.54	2.8396	18	16.12
600	22.547	2.010	0.46	2.8432	21	14.48
650	22.504	2.014	0.46	2.8482	21	12.10
700	22.443	2.019	0.44	2.8556	22	8.64

Fig. 5 shows the frequency dependence of the real part of the complex initial permeability for as-cast and annealed sample in the temperature range 300 to 600 $^\circ\text{C}$ for 30 minutes at a fixed frequency of 1 kHz. The curve reveals the strong dependence of initial permeability on annealing temperature, when annealed at temperature below the onset of crystallization. An increase of μ' with T_a from 300 to 475 $^\circ\text{C}$ is observed due to irreversible structural relaxation of the amorphous matrix. At $T_a = 500^\circ\text{C}$, the permeability sharply drops to a lower value. This is the temperature around which initiation of crystallization takes place as found by DTA and XRD. The decrease of permeability may be attributed to the new stresses developed in the matrix by the growing crystallites, which act as pinning centers for the domain walls constraining the domain wall mobility as well as weak inter-grain magnetic coupling since the growing crystallites are far apart from each other representing small volume fraction that cannot be exchange coupled and the anisotropy cannot be averaged out (Hakim and Manjura 2004, Maria *et al.* 2011). Further increase of annealing temperature leads to the increase of permeability due to the increase of volume fraction of α -Fe(Si) nanograins coupled via exchange interaction resulting in a reduction of anisotropy energy. The trends of increasing low frequency permeability exist up to 575 $^\circ\text{C}$, i.e. maximum permeability corresponding to the best soft magnetic properties is observed at this temperature. A large enhancement of μ' was observed above the annealing temperature of $T_a = 575^\circ\text{C}$, μ' drops to lower value radically. The probable reason might be the evaluation of boride

phase having high anisotropy energy as well as large grain size which attains a value of 21 nm at $T_a = 600^\circ\text{C}$. This may leads to the increase of anisotropy energy to a high value, which essentially reduces the local exchange correlation length weakening the intergranular magnetic coupling as a result of which magnetic hardening takes place (Hasiak *et al.* 2000, Jing *et al.* 1996). The boride phase has been detected by our XRD experiment above 600°C .

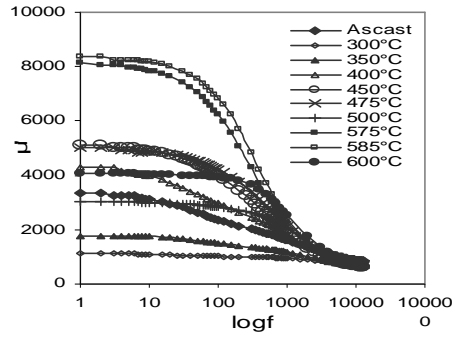


Fig. 5. Frequency dependence of μ' at different T_a for 30 minutes of $\text{Fe}_{74}\text{Cu}_{0.5}\text{Nb}_3\text{Si}_{13.5}\text{B}_9$ alloy.

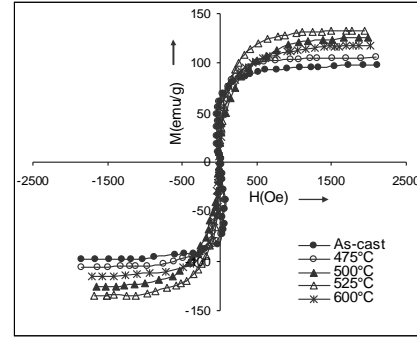


Fig. 6. Specific magnetization versus magnetic field of as-cast and annealed samples of $\text{Fe}_{74}\text{Cu}_{0.5}\text{Nb}_3\text{Si}_{13.5}\text{B}_9$ alloy.

Fig. 6 shows the field dependence of specific magnetization for amorphous as-quenched and thermally treated samples measured by VSM. It can be seen that with increasing annealing temperature magnetization increases until $T_a = 525^\circ\text{C}$. Aranda *et al.* (1998) have studied the approach to saturation in nanocrystalline FINEMET materials. The magnetization prior to saturation is associated with reversible rotation and has been fitted to the law

$$M(H) = M_s \left[1 - \frac{a_1}{H} - \frac{a_2}{H^2} \right] + bH^{1/2}, \quad (2)$$

where the term $\frac{a_2}{H^2}$ was described as being a direct consequence of the random anisotropy model, and attributable to Fe-Si grains. The co-efficient a_2 reflects the Herzer's predicted effective magnetic anisotropy of the nanocrystalline material, where as in amorphous alloys it is postulated as being caused by local stress and magneto elastic coupling.

Saturation magnetization M_s has been observed to increase with the increase of annealing temperature. An increase of M_s for the annealed samples at 450 to 525°C is due to the irreversible structural relaxation, changing the degree of chemical disorder of the amorphous state (Lovas *et al.* 2000) and enhanced volume fraction of Fe(Si) nanocrystals that are exchange coupled. The saturation magnetizations are shown in Table 3.

Table 3. The values of saturation magnetization of $\text{Fe}_{74}\text{Cu}_{0.5}\text{Nb}_3\text{Si}_{13.5}\text{B}_9$ alloys at different annealing temperature with constant annealing time 30 minutes.

Samples	Annealing temperature, T_a in $^{\circ}\text{C}$	Saturation magnetization, M_s in emu /gm
	As-cast	128
$\text{Fe}_{74}\text{Cu}_{0.5}\text{Nb}_3\text{Si}_{13.5}\text{B}_9$	475	133
	500	138
	525	141
	600	124

A rapid decrease in M_s has been observed with increasing annealing temperature at 600°C for $\text{Fe}_{74}\text{Cu}_{0.5}\text{Nb}_3\text{Si}_{13.5}\text{B}_9$. The decreasing of M_s may be connected with the enrichment of the residual amorphous phase with Nb that weakens the coupling between ferro-magnetic nanograins (Berkowitz *et al.* 1981). Also the role of Si diffusion into Fe (Si) nanograins and these local environments also may have effect in decreasing M_s . The decrease of M_s for the sample higher annealing temperature on ordering of Fe_3Si nanograin can not be ruled out.

CONCLUSION

Nanocrystalline amorphous ribbons of the Finemet family with nominal composition $\text{Fe}_{74}\text{Cu}_{0.5}\text{Nb}_3\text{Si}_{13.5}\text{B}_9$ have been studied to find out the correlation between microstructural features and soft magnetic properties as dependent on various stages of nanocrystallization during the isothermal annealing around the crystallization temperature of their amorphous precursors. DTA reveals the primary, Fe(Si) and secondary (Fe-B) crystallization temperatures with the manifestation of two well-defined exothermic peaks. Magnetic initial permeability of nanocrystalline/amorphous ribbon strongly depends on annealing temperature. The improvement in the soft magnetic properties can be ascribed to the much refined grain structure in the range of 10 to 20 nm obtained at various temperatures during annealing. When alloys were annealed for 30 minutes at various temperatures, the maximum initial permeability (μ') were observed at $T_a = 575^{\circ}\text{C}$. The saturation magnetization for nanocrystalline samples has slightly increased for annealing at temperature around the onset of crystallization. When annealed at higher temperature at which complete crystallization takes place, magnetization decreases again.

ACKNOWLEDGMENTS

The authors gratefully acknowledge Dr. Dilip Kumar Saha of Material Science Division, Atomic Energy Centre, Dhaka for his help in XRD measurements.

REFERENCES

- Aranda, G. R., J. Gonzalez, and K. Kulakowski. 1998. Approach to the magnetic Saturation in Nanacrystalline Ferromagnets in the random anisotropy model. *J. Appl. Phys.* **83**: 6341-6344.

- Berkowitz, A. E., J. L. Walter and K. F. Wall. 1981. Magnetic properties of amorphous particles produced by Spark Frosion. *Phys. Rev. Lett.* **46**: 1484-1486.
- Bigot, J., N. Lecaude, J. C. Perron, C. Millan, C. Ramiarinjaona and J. F. Riolland. 1994. Influence of Annealing Conditions on Nanocrystalization and Magnetic Properties in Fe_{73.5}Cu₁Nb₃Si_{13.5}B₉ alloy. *J. Magn. Magn. Mater.* **133**: 299-303.
- Hakim M. A. and S. Manjura Hoque, (2004), "Effect of structural parameters on soft magnetic properties of two phase nanocrystalline alloy of Fe_{73.5}Cu₁Ta₃Si_{13.5}B₉", *J. Magn. Magn. Mater.* **284**: 395-402.
- Hasiak, M., J. Zbroszczyk, J. Olszewki, W. H. Ciuzynska, B. Wyslocki and A. Blachowicz. 2000. Effect of cooling rate on Magnetic Properties of Amorphous and Nanocrystalline Fe_{73.5}Cu₁Nb₃Si_{15.5}B₇ alloy. *J. Magn. Magn. Mater.* **410**: 215-216.
- Herzer, G. 1989. Grain Structure and Magnetism of Nanocrystalline Ferromagnets, *IEEE Trans. Magn.* **25**: 3327-3328.
- Jing Zhi, Kai-Yuan He, Li-Zhi Cheng, Yu-jan Fu. 1996. Influence of the elements Si/B on the Structure and Magnetic Properties of Nanocrystalline (Fe, Cu, Nb) _{77.5}Si_x B_{22.5-x} alloys. *J. Magn. Magn. Mater.* **153**: 315-317.
- Lovas, A. , L. F. Kiss, and I. Balong. 2000. Saturation magnetization and amorphous Curie point changes during the early stage of amorphous-nanocrystalline transformation of a FINEMET-type alloy. *J. Magn. Magn. Mater.* **463**: 215-216.
- Manjura, S. Hoque and M. A. Hakim. 2007. Ultra-Soft magnetic properties of devitrified Fe_{75.5}Cu_{0.6}Nb_{2.4}Si₁₃B_{8.5}. *J. Materials Chemistry and Physics* **101**: 112-117.
- Maria, K. H., Shiba P. Mondal, Shamima Choudhury, S. S. Sikder, M. A. Hakim and D. K. Saha. 2011. Effect of Annealing Temperature on the soft magnetic Properties of Fe_{75.5}Cu₁Nb₁Si_{13.5}B₉ Amorphous Alloys. *Journal of Emerging Trends in Engineering and Applied Sciences* **2**(1): 102-108.
- Noh, T. H., M. B. Lee, H. J. Kim and I. K. Kang. 1990. Relationship between crystallization process and magnetic properties of Fe-(Cu-Nb)-Si-B amorphous alloys. *J. Appl. Phys.* **67**: 5568.
- Rubinstein, M., V. G. Harris and P. Lubitz. 2001. Ferromagnetic resonance innanocrystalline Fe_{73.5}Cu₁Nb₃Si_{13.5}B₉ (Finemet). *J. Magn. Magn. Mater.* **234**: 306-308.
- Yoshizawa, Y. and K. Yamachi. 1990. Fe-based soft magnetic alloys composed of ultrafine grain structure. *Mater. Trans. JIM.* **31**: 307-308.
- Yoshizawa, Y. and K. Yamachi. 1991. Magnetic properties of Fe-Cu-M-Si-B (M = Cr, V, Mo, Nb, Ta, W) alloy. *Mater. Sci. Eng. A.* **33**: 176-179.
- Yoshizawa, Y., S. Oguma and K. Yamauchi. 1988. New Fe-Based Soft Magnetic Alloys Composed of Ultra fine Grains Structure. *J. Appl. Phys.* **64**: 6044-6047.

(Received revised manuscript on 10 July, 2011)